High performance supercapacitor was achieved with the electrode of hybrid material of Nitrogen functionalized graphene with polyaniline

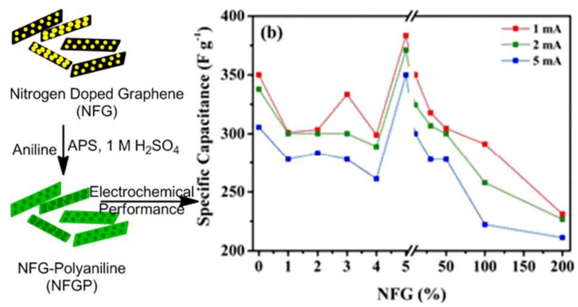

RSC Advances

ARTICLE

Hybrid composite of nitrogen functionalized graphene-polyaniline electrode for high performance supercapacior

Received 00th January 20xx,
Accepted 00th January 20xx

DOI: 10.1039/x0xx00000x

www.rsc.org/

M. Umashankar and S. Palaniappan[a]

Polyaniline (PANI) hybrid composite was prepared with nitrogen functionalized graphene (NFG) via in-situ polymerization of aniline in presence of NFG for supercapacitor electrode. Nitrogen functionalized graphene-polyaniline composite (NFGP) was used as electrode in symmetric supercapacitor cell configuration and evaluated its performance by cyclic voltammetry, charge-discharge and electrochemical impedance spectroscopy measurements. The electrochemical performances of NFGP are compared with its constituents of NFG, PANI and also with hydrothermal treated graphene oxide (HTGO). Electrochemical capacitance of PANI (350 F g^{-1}) increased with increase in the amount of NFG, attained a maximum with 5 wt. % of NFG (383 F g^{-1}) and then decreased with further increase of NFG. PANI with 5 wt. % NFG showed a high discharge capacitance value of 383 F g^{-1} with energy density (19 W h kg^{-1}) at a power density of 200 W kg^{-1}. Initial capacitance of NFGP5 cell value decreases to 253 F g^{-1} up to 700 charge-discharge cycles and then almost remained constant up to 33000 cycles (~240 F g^{-1}). Moreover, NFGP5 electrode showed a very low ESR value (0.6 Ω), low time constant (0.1 ms) and phase angle 82° close to that of ideal capacitor value of 90°. NFGP5 sample was thermally stable up to 250 °C. Hydrophilicity of NFGP5 was higher compared to that of PANI. Morphological analysis revealed the uniform distribution of PANI on the surface of NFG, indicating strong interaction between them.

1. Introduction

Supercapacitors (SCs), also called electrochemical capacitors or ultracapacitors, are the energy storage devices intermediate to that of batteries and conventional capacitors in terms of energy and power densities; and aroused a broad interest due to their potential applications in portable electronic devices, power backup systems, hybrid electric vehicles, and medical devices [1-3]. Depending upon the charge storage mechanism, the supercapacitors are categorised into two types i.e., electrochemical double layer capacitors (EDLC) and pseudo capacitors (PC). Performance of the SCs highly depends on the properties of electrode materials; Carbon materials exhibit EDLC whereas functionalized carbons, conducting polymers and metal oxides exhibit pseudo capacitive properties.

Among the various electrode materials available for SCs, polyaniline (PANI) has attracted much attention due to its good conductivity, high redox reversibility, relatively cheap, easy synthesis, eco-friendly, proven to be one of the promising electrode materials in supercapacitors, and large variety of applications such as electrochromic devices, secondary batteries, catalysis, electrostatic discharge protection etc [3, 4]. However, the main drawback of polyaniline application as supercapacitor electrode is connected with its poor stability during cycling. To overcome these drawbacks, there is a new tendency to synthesize composite hybrid materials combining two or more pure materials as electrode materials. [5-10]

Graphene is proposed as the next generation electrode material for supercapacitors owing to its attractive properties such as high surface area (2630 $m^2 g^{-1}$), high thermal conductivity (~5000 W mK^{-1}), fast charged carrier mobility (~200 000 $cm^2 V^{-1} s^{-1}$) and strong Young's modulus (~1 TPa), chemical stability, and tunable band gap [11, 12]. Recently N-functionalized graphenes have shown to exhibit enhanced charge storage ability compared to unmodified graphene counter parts. Heteroatoms on carbon surfaces dramatically enhance the specific capacitance values of carbon materials by pseudo capacitive effects [12-15]. Hence, the use of nitrogen functionalized graphene having high-surface area, good electrical, mechanical properties, superb thermal stability and increased electrolyte wettability properties will provide additional advantages for the polyaniline electrode in energy storage. Literature reports on the use of NFG and its composite with PANI as electrode material in supercapacitor is given in Table 1.

Herein, we report the facile synthesis of NFGP via in-situ polymerization of aniline in presence of NFG. The NFGP composite is then subjected to morphology, thermal, elemental analysis, and electrochemical studies (cyclic voltammetry, charge-discharge and electrochemical impedance spectroscopy). The results of the composite are compared with its individual components of HTGO, NFG and PANI.

[a] Polymers& Functional Materials Division, CSIR – Indian Institute of Chemical Technology, Tarnaka, Hyderabad 500 007, Telangana, India
Email: palani74@rediffmail.com, palaniappan@iict.res.in
Phone: +91-40-27191474, Fax: +91-40-27193991.

Table 1. Literature reports on electrochemical performance of nitrogen doped graphene and it's composite with polyaniline

Ref	Electrode Material	Nitrogen Source	Nitrogen %	Electrolyte	Configuration (Two/Three electrode)	Capacitance ($F\ g^{-1}$)
5	NCNT-PANI	Ammonia	---	0.1 M Na_2SO_4	Three	250
6	NFG	Urea	5.6	1 M KOH	Two	45.2
6	NFG-PANI	Urea	5.6	1 M KOH	Two	145.9
15	NFG	PANI + PS	8.7	6 M KOH	Three	381
16	NFG	Ammonium Carbonate	6.8-10.1	6 M KOH	Three	295
17	NFG	Nitrogen plasma	1.68-2.51	1 M $TEABF_4$	Two	280
18	NFG	Ethylene diamine	9.83	1 M H_2SO_4	Three	365
19	NFG	ammonia	2	1 M $TEABF_4$	Two	145
20	NFG	Urea	10.13	6 M KOH	Three/Two	326/56
21	NFG	Dicyandiamide	---	1 M H_2SO_4	Three/Two	190/52
22	NFG	dicyandiamide	9.96	6 M KOH	Two	302
23	NFG	Urea	3.95-6.61	6 M KOH	Three	308
24	NFG	Ammonia	5	1 M H_2SO_4	Three	9.5 mF cm^{-2}
25	NFG	p-Phenylenediamine	10.85	6 M KOH	Two	313
26	NFG	Melamine	26	2 M H_2SO_4	Three	343

2. Experimental

2.1. Materials

Aniline [S. D. Fine Chemicals, India] was vacuum distilled prior to use. Ammonium persulfate (APS), sulfuric acid (H_2SO_4) [Rankem, India], graphite, ethylenediamine [Sigma Aldrich, USA] were used as received. All the reactions were carried out with distilled water and solvents.

2.2. Preparation of Nitrogen Functionalized Graphene (NFG):

Graphite oxide was synthesized from natural graphite powder by following the procedure reported by Chen et al. [27] NFG was synthesized by following the reported procedure [18]. Briefly, 2.5 mL of ethylenediamine, and 150 mL of GO (10 mg mL^{-1}) suspensions were mixed in a beaker and ultrasonically stirred for 0.5 h, then transferred into a 250 mL stainless steel autoclave. Hydrothermal treatment of this mixed solution was made at 180 °C for 10 h. After hydrothermal treatment autoclave was naturally cooled to room temperature, the as-prepared black product was then washed with distilled water and acetone in order to remove residual unreacted compounds. Finally, the sample was dried in an oven at 60 °C.

2.3. Preparation of Hydrothermally Treated Graphene Oxide (HTGO):

HTGO was prepared by following the above procedure of NFG, i.e. hydrothermal treatment on GO without the use of ethylene diamine.

2.4. Preparation of Nitrogen Functionalized Graphene - Polyaniline composites (NFGP):

Series of NFG polyaniline composites were prepared by aqueous polymerization of aniline using APS oxidant by changing the ratio of aniline and NFG in the reaction mixture. In a typical procedure, particular amount of NFG was dispersed in a 50 mL of 1 M H_2SO_4 solution containing aniline by ultra-sonication using bath sonicator for 0.5 h. Oxidant solution was prepared by dissolving a calculated amount of APS in 50 mL of 1 M H_2SO_4 solution. The oxidant solution was added to the NFG-aniline mixture and the mixture was constantly stirred for 4 h. at ambient temperature. Then, the reaction mixture was filtered under vacuum, washed with ample amount of distilled water and acetone until the filtrate was colourless. The obtained powder was dried in an oven at 60 °C till a constant mass.

For comparison, polyaniline (PANI) was prepared by the same procedure without the use of NFG.

2.5. Preparation of electrode and supercapacitor cell

Working electrodes were prepared by pressing the samples on stainless steel mesh (316 grade) with the application of 6 tons of pressure without any binder. Symmetric supercapacitor cell in the form of two-electrode Swagelok type was constructed using two working electrodes separated by absorptive glass mat separator in 1 M H_2SO_4 electrolyte (Inset : Fig. 3a).

3. Instrumentation

X-ray photoelectron spectroscopy (XPS) measurements were carried out on an Kratos Axis Ultra DLD spectrometer (Kratos Analytical, UK) equipped with a monochromator alumina source (Alkα, *hv*=1486.6 eV). Morphology studies of the polymer powder samples were carried out with a Hitachi S-4300 SE/N field emission scanning electron microscope (FESEM) (Hitachi, Tokyo, Japan) operated at 20 kV. The polymer powder sample was sputtered on a carbon disk with the help of double-sided adhesive tape. Transmission electron microscopy (TEM) measurement was carried out with Hitachi S-5500 instrument operated at an accelerate voltage of 30 kV. The sample was prepared by casting sample dispersion on carbon-coated copper grids (300 mesh) and allowed to dry at room temperature. Water contact angles for the samples in pellet form were recorded with a contact angle analyzer (G10), Kruss, Germany) to check the surface compatibility of the samples with the aqueous electrolyte. Thermogravimetric analysis (TGA) was performed with TGA Q500 Universal (TA Instrument, UK) at a heating rate of 10 °C min^{-1} from ambient temperature to 700 °C under nitrogen atmosphere. All the electrochemical tests on supercapacitor cell were carried at ambient temperature using ZIVE MP5 multichannel electrochemical workstation (WonATech Co., Ltd., Korea). Cyclic voltammograms (CV) were recorded at various sweep rates and charge-discharge experiments were carried out at various currents. Electrochemical impedance spectroscopy EIS measurement was performed at a DC bias of 0 V with a sinusoidal signal of 10 mV amplitude over the frequency range of 40 kHz to 10 mHz.

4. Results and discussion

The aim of the present work is to improve the pseudo capacitive performance of polyaniline (PANI) electrode via the incorporation of nitrogen functionalized graphene (NFG) to polyaniline. Heteroatom functionalized carbon has been used as a support materials for conducting polymers due to enhanced charge storage ability, chemical stability, excellent electrical conductivity, increased electrolyte wettability, large theoretical surface area and mitigate the cycle degradation issues that are caused by mechanical problems. NFG powder sample was prepared by the hydrothermal treatment of graphene-oxide (GO) using ethylene diamine as a nitrogen precursor. For comparison purpose, GO was subjected for hydrothermal treatment (HTGO) without using ethylene diamine. XPS was performed to analyse the chemical composition of HTGO and NFG (Fig. 1). HTGO exhibits the peaks of C 1s, and O 1s at 285 and 534 eV with atomic percentages of 82 and 18% respectively, whereas, the NFG show C 1s, N 1s, and O 1s peaks at 285, 401 and 532 eV with corresponding atomic percentages of C (89%), N (5%), O (6%). The presence of O 1s peak in HTGO and NFG shows that the oxygen is not completely removed in the hydrothermal process. Further, the presence of nitrogen element on NFG was confirmed from elemental analysis. The CHNS data of NFG material show the presence of 8 wt. % nitrogen. This result also supports the presence of nitrogen in NFG.

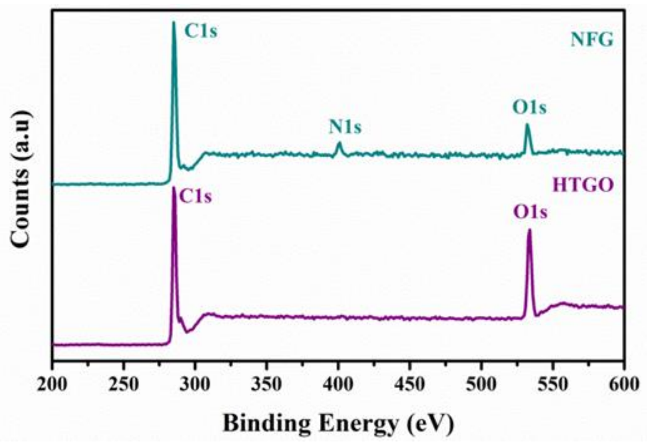

Figure 1. XPS spectra of HTGO and NFG.

After the confirmation of formation of NFG, to improve the electrochemical performance of PANI, hybrid composites were prepared via chemical oxidative polymerization of aniline using ammonium persulfate oxidant with various amounts of NFG, i.e., 1, 2, 3, 4, 5, 10, 30, 50, 100 and 200 wt. % w.r.t aniline and the corresponding NFGP composites are labeled as NFGP1, NFGP2, NFGP3, NFGP4, NFGP5, NFGP6, NFGP7, NFGP8, NFGP9, and NFGP10 respectively.

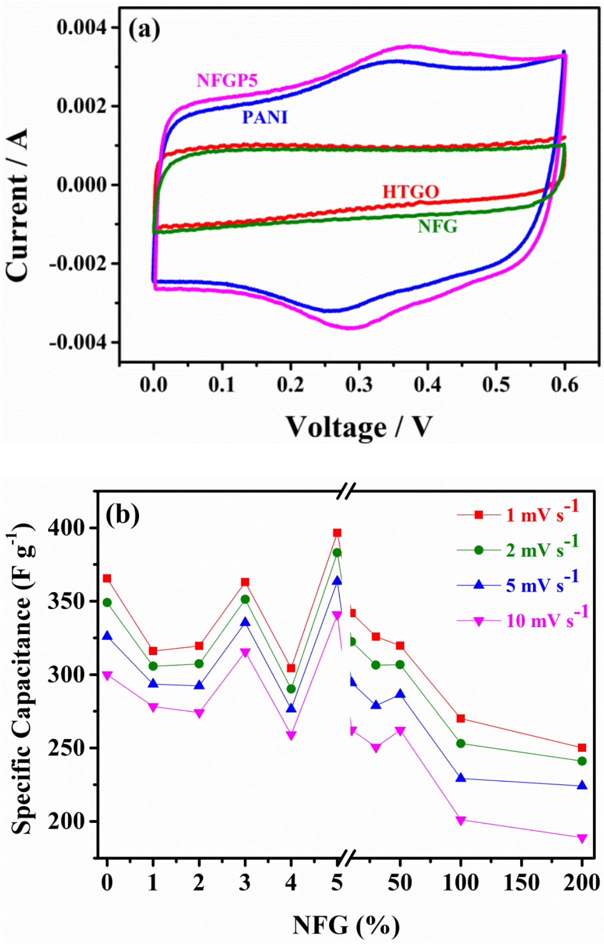

Figure 2. **(a)** Cyclic voltammograms of HTGO, NFG, PANI and NFGP5 supercapacitor cells in 1 M H_2SO_4 solution measured at sweep rate of 5 mV s^{-1}. **(b)** Effect of NFG in NFGP composites and their specific capacitance at various scan rates.

To evaluate the electrochemical characteristics of the hybrid samples, cyclic voltammetry as well as charge-discharge studies were performed for PANI-NFG materials in two electrode symmetric cell configuration using 1 M H_2SO_4 electrolyte and AGM as a separator. The results are compared with the cells of HTGO, NFG and PANI. As a representative system, the cyclic voltammograms recorded at a sweep rate of 5 mV s^{-1} for HTGO, NFG, PANI, and NFGP5 are represented in Fig. 2a. It is observed from the figure that the voltammograms are almost rectangular with good symmetry, showing a good capacitive behaviour of the electrode materials. Observation of a small hump in the voltammograms of PANI and NFGP5 indicates that the pseudo capacitative process is associated with EDLC process. Specific capacitance from cyclic voltammogram (CV-Cs) with respect to one electrode was calculated using the formula, CV-Cs= $(4*Q*1000)\ (\Delta V*m)^{-1}$, where Q is the average charge from anodic and cathodic curves, ΔV is voltage window and m is the mass of the active material in two electrodes. The results show that the NFG has higher capacitance compared to HTGO and this is due to the incorporation of electrochemically active functional groups on the graphene sheets [18]. The presence of heteroatoms could effectively enhance the surface activity and electrochemical performance of the carbons due to the conjugation between the lone-pair electrons and the π-system of the carbon framework. The values obtained for NFG in the present study are higher than the values reported in the literature. [Table 1 - Refs. 6, 19-21]

The effect of NFG loading and sweep rates on CV-Cs in PANI and NFGPs is represented in Fig. 2b. From the figure it is observed that the NFGP5 composite with 5 wt. % NFG loading showed better capacitance among all other composites and also pristine PANI at all measured scan rates. The specific capacitance value of all the samples decreases as the scan rate increases. The reason may be that, at lower currents, the ions have enough time to diffuse into the inner surfaces of electrode materials while at the high currents the ions can only partially penetrate into the inner surfaces. NFGP5 gave the highest CV-Cs of 397 F g^{-1} at 1 mV s^{-1} and the CV-Cs value decreased either with an increase or decrease in the amount of NFG in NFGP composites. A similar trend was also observed with other sweep rates i.e., 5 and 10 mV s^{-1} (Fig. 2b). The increase in CV-Cs with increase in the amount of NFG (1 to 5 wt. %) is expected to the well dispersion of NFG particles in NFGP composite their by facilitating the migration and diffusion of the electrolyte ions during the fast charge/discharge process and leading to effective utilization of electrode materials that contributes the total capacitance. Further increase of NFG (> 5 wt. %) decreases the CV-Cs due to the incorporation of relatively less electrochemically active NFG compared to PANI in the NFGP composite material. Addition of a small amount of NFG i.e., 5 wt. % is sufficient to enhance the performance of PANI by synergistic effects of PANI and NFG.

Charge-discharge (CD) experiments were carried out for NFG, HTGO, PANI and NFGP symmetric cells at different applied currents. The CD curves recorded at an applied current of 1 mA is shown in Fig. 3a, the curves are nearly linear and symmetric, also with less internal resistance (*iR* drop), which are characteristics of a good capacitor. As the electrochemical capacitance is proportional to the discharge time of CD curves, from figure the discharge time of NFG is larger than HTGO, indicating that the introduction of nitrogen improves the capacitance of electrodes. Moreover, the discharge times of PANI and NFGP5 are greater than those of NFG and HTGO indicating the main capacitive performance of the electrodes are due to pseudo capacitive behavior.

Specific capacitance from charge-discharge measurement (CD-C_s) was calculated using the following equation [28] CD-C_s = $(4*i*\Delta t)(\Delta V*m)^{-1}$, where i is the constant discharge current, Δt

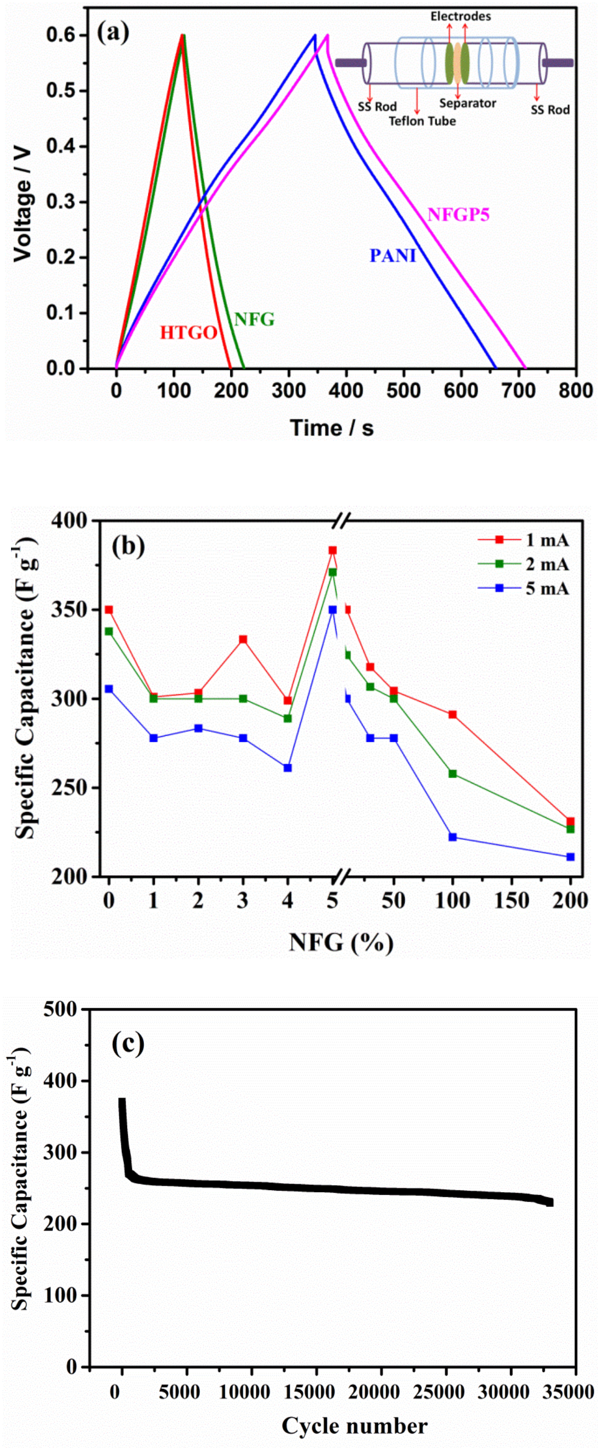

Figure 3. (a) Galvanostatic Charge-discharge curves of HTGO, NFG, PANI and NFGP5 supercapacitor cells in 1 M H_2SO_4 solution measured at 1 mA current (Inset : Construction of symmetric supercapacitor cell). **(b)** Effect of NFG in NFGP composites and their specific capacitance at various applied currents and **(c)** Specific capacitance versus cycle number of NFGP5 supercapacitor cell in 1 M H_2SO_4.

is the discharge time, ΔV is the voltage window during discharge (neglecting *iR* drop), *m* is the mass of the active material in both electrodes. CD-C_s also shows similar trend as CV-Cs, wherein NFG shows higher capacitance than HTGO. The effect of NFG loading and applied currents on CD-Cs in PANI and NFGPs is represented in Fig. 3b. From the figure it is observed that the NFGP5 composite with 5 wt. % NFG loading showed better capacitance among all other composites and also pristine PANI at all measured currents and is in accordance with the results observed from CV-Cs values.

Among the NFGP composites, higher specific capacitance is observed for NFGP5 from both CV and CD analysis. Hence, further characterization is done for NFGP5 symmetric supercapacitor. Furthermore, the specific capacitance of NFGP5 is higher than the values reported by Wang et al. for Nitrogen doped graphene PANI (160.2 F g^{-1}) [6] and by Haq et al. for Nitrogen doped CNT-PANI (250 F g^{-1}) [5].

Energy density and power density are the two important performance indicators for energy storage devices. Notably, the NFGP5 symmetric supercapacitor can deliver a high energy density of 19 W h kg^{-1} at a power density of 200 W kg^{-1}, and the energy density still retains 17 W h kg^{-1} with a higher power density of 1000 W kg^{-1}.

Long cycling life is an important requirement for practical performance of supercapacitors. The cycling life test for NFGP5 cell was performed by constant CD cycling at 2 mA in 1 M H_2SO_4. Fig. 3c shows the cycling behavior of supercapacitors for 33000 cycles. It is observed that the specific capacitance of NFGP5 cell decreases for the first 700 cycles and then remained constant. The initial decay in capacitance with cycle number is due to the repetitive volumetric expansion/contraction of PANI chains during the continuous injection/rejection (charge/discharge) of electrolyte ions, deteriorating the charge distribution and conformation of π conjugated PANI chains. After initial degradation, the further degradation is inhibited by the mechanical support given by NFG framework. A similar cycle degradation patterns were reported in several publications in the literature [29-31].

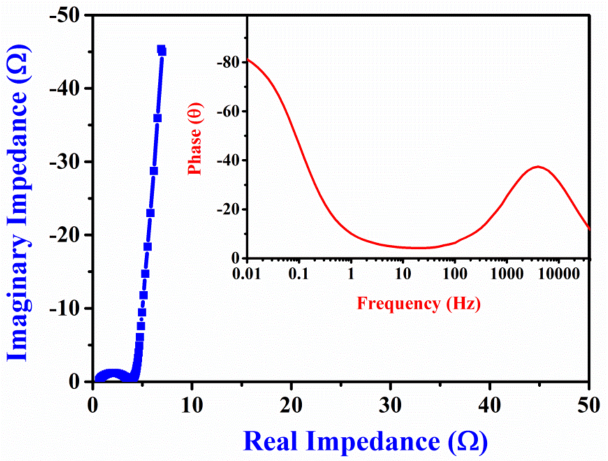

Figure 4. Nyquist plots of NFGP5 supercapacitor cell (Inset: bode plot).

Electrochemical Impedance Spectroscopy *(*EIS) is an important analytical technique used to gain information about the characteristic frequency responses of supercapacitors and the capacitive phenomena occurring in the electrodes. Fig. 4 represents the Nyquist plot of NFGP5 symmetric cell in the frequency range of 40 kHz to 10 mHz measured at 0 V and an amplitude of ±10 mV and the corresponding bode plot is shown as an inset in Fig. 4. The nyquist diagram of supercapacitor cell show two distinct regions, i.e., a depressed semicircle in the high-frequency range corresponds to the electron-transfer limited process and a linear portion with a slope close to unity in the low-frequency range. The appearance of a straight line in the low frequency region was an indication of good ion diffusion at the interface between the electrolyte and electro-active materials, suggesting ideal supercapacitive behavior. The high frequency intercept on the real axis provides the magnitude of equivalent series resistance (ESR). The observation of low resistance was also confirmed from the negligible voltage drops at the beginning of the discharge curves in charge-discharge curves. In the present case the value of ESR was obtained as 600 mΩ, which is lower than that of the normal value, i.e. in ohms. Diameter of the semicircle provides the charge transfer resistance (R_{ct}) and was found to be 3 Ω. This result indicates the good charge transfer in the electrolyte–electrode interface and is due to the conducting nature of NFGP. The time constant was calculated from the maximum of the semi-circle appeared in the high frequency region and was found to be 0.1 ms, which ensure fast charge-discharge characteristics that are preferred for electrochemical supercapacitors [32]. The specific capacitance (EIS-*Cs*) from EIS was calculated from the imaginary part of the complex impedance according to the equation [8],

$$EIS - Cs = 2/(2\pi f Z_{im} m)$$

Where f is the frequency, Z_{im} is the imaginary part of complex impedance at frequency f and m is the mass of materials in one electrode. The factor of 2 comes from the fact that the overall capacitance measured from the test cells is the addition of two equivalent single-electrode capacitors in series. The EIS-*Cs* for NFGP5 was found to be 234 F g^{-1}. From the bode diagram it can be observed that the phase angle value of NFGP5 is ~82°; which is closer to that of an ideal capacitor 90°. These result of low ESR, low charge-transfer resistance, low time constant, high phase angle and good specific capacitance suggest the better electrochemical characteristics of PANI-NFG composite for supercapacitor.

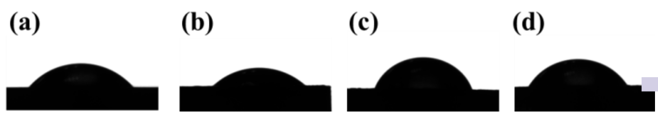

Figure 5. Digital images of water droplet on the surfaces of (a) HTGO, (b) NFG, (c) PANI and (d) NFGP5

The digital images for the water contact angle measurements are shown in Fig. 5. HTGO showed contact angle of 48.9° and the contact angle decreased to 41.9° (NFG) with the introduction of nitrogen in HTGO. The introduction of nitrogen in HTGO increases the hydrophilicity. Generally, increase in hydrophilicity increases the electrochemical performances [33, 34]. In order to find this behaviour, we measured the contact angle of PANI and NFGP5 composite. NFGP5 composite showed lower value of contact angle (57.2°) compared to that of PANI (64.4°). This result indicates that the hydrophilicity of PANI increases with the use of NFG in NFGP5, which assist more electrolyte accessibility to the electrode and results in higher electrochemical performance than PANI.

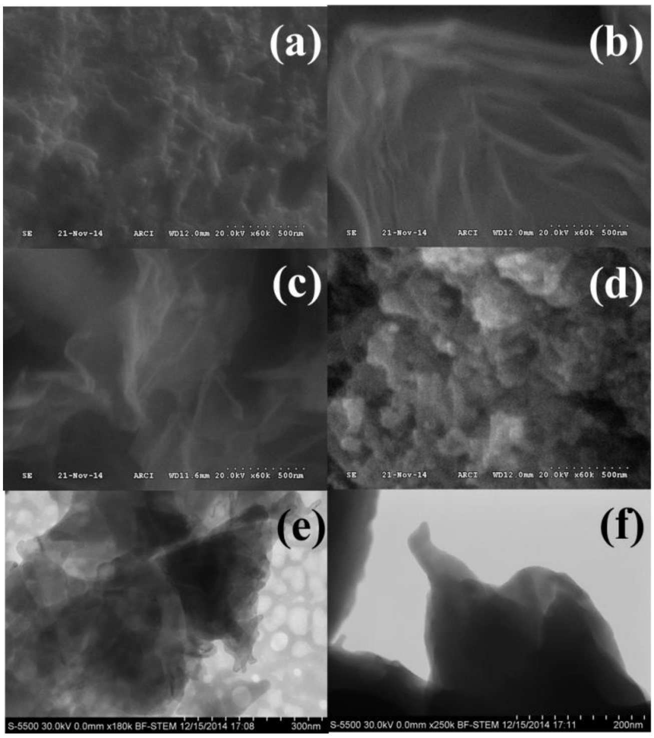

Figure 6. FESEM images of (a) PANI, (b) NFG, (c) HTGO, (d) NFGP5 and (e, f) TEM images of NFGP5.

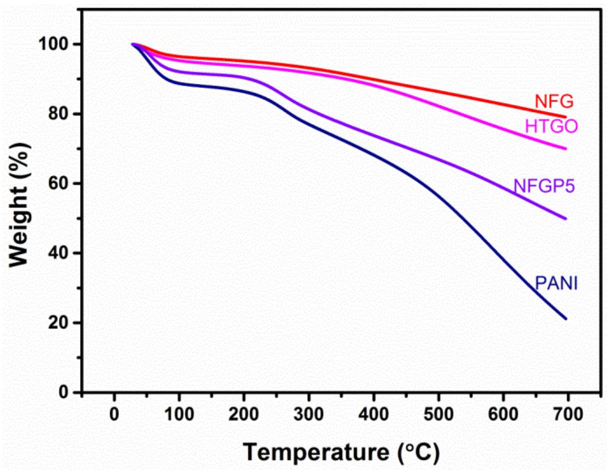

Figure 7. TG thermograms of PANI, NFG, HTGO and NFGP5.

Surface morphologies of PANI, HTGO, NFG and NFGP5 samples were found from FESEM and the images are shown in Fig. 6. PANI shows fibrous morphology, whereas FESEM picture of HTGO and NFG shows randomly distributed, overlapped and loosely stacked layered morphology. The exfoliation is more in NFG compared to HTGO. NFGP5 composite material shows agglomerated nano fibrous morphology of PANI. During the synthesis of NFGP5 hybrid composite, the aniline monomers are adsorbed on surfaces of the NFG via π-π conjugation and chemical bonding effects. The adsorbed aniline molecules act as nucleation sites and the polymerization took place preferentially and continuously near the adjacent NFG layers resulting in agglomerated structures, further the enclosed NFG also provides the rigid support during the repetitive charge-discharge cycling of NFGP5 supercapacitor cell. The nanostructured electrodes have many advantages, such as higher electrode/electrolyte contact area, leading to higher charge/discharge rates, and short path lengths for electronic and electrolyte transport, thus allowing for the improved utilization of electrode materials. TEM images of NFGP5 shows the better exfoliation of graphene layers and covering of PANI on graphene layers.

Thermogravimetric thermograms of HTGO, NFG, PANI, NFG and NFGP5 are depicted in Fig. 7. In the initial step, small weight loss behaviour was observed for both hydrothermal graphene oxide and nitrogen functionalized graphene. This initial weight loss observed up to 110 °C is due to the escape of physically adsorbed water molecule. Weight loss observed from 110 to 500 °C was 13 and 10 wt. % for HTGO and NFG respectively. This result indicates that nitrogen functionalization on heat treated graphene oxide increases the thermal stability of HTGO. Thermal stability of polyaniline carbon composite of NFGP5 is compared with the thermal stability of PANI and NFG. The observations are : (i) TGA thermograms of PANI, NFG and NFGP5 show initial weight loss behaviour up to 110 °C due to escape of water molecules , (ii) Both PANI and NFGP5 are stable up to 250 °C and (iii) in the weight loss range from 110 to 550 °C (a) NFGP5 underwent 29% weight loss, whereas, PANI underwent 41%. This higher stability in the case of NFGP5 is due to the presence of stabile NFG in NFGP5, (b) NFGP5 is less stable than NFG and this lower stability of NFGP5 indicates the presence of PANI. These stability behaviours indicate the presence of both PANI and NFG in NFGP5 composite.

Conclusions

The electrochemical performances of hybrid composite of NFG-PANI are compared with its constituents of NFG, PANI and also with hydrothermal treated graphene oxide (HTGO). The important results of hybrid composite (NFGP) supercapacitor are: specific capacitance value of hybrid composite is higher than that of its individual components; very low ESR value (0.6 Ω), low time constant (0.1 ms) and phase angle 82° closer to that of ideal capacitor value of 90°. This hybrid composite material is a suitable electrode for supercapacitor application.

Acknowledgements

We thank Department of Science & Technology, New Delhi for funding under the project (DST/TSG/PT/2011/179-G). We are thankful to Dr. M. Lakshmi Kantam, Director CSIR-IICT for his support and encouragement. Umashankar Male is thankful to CSIR, India for financial assistance.

References

1 Y. Zhang, H. Feng, X.B. Wu, L.Z. Wang, A.Q. Zhang, T.C. Xia, H.C. Dong, X.F. Li and L.S. Zhang, *International Journal of Hydrogen Energy*, 2009, 34, 4889.
2 G.P. Wang, L. Zhang and J.J. Zhang, *Chemical Society Review*, 2012, **41**, 797.
3 G.A. Snook, P. Kao and A.S. Best, *Journal of Power Sources*, 2011, **196**, 1.
4 G. Ciric-Marjanovic, *Synthetic Metals*, 2013, **177**, 1.
5 A. Ul Haq, J. Lim, J.M. Yun, W.J. Lee, T.H. Han and S.O. Kim, *Small*, 2013, **9**, 3829.
6 W. Wang, Q. Hao, W. Lei, X. Xia and X. Wang, *Journal of Power Sources*, 2014, **269**, 250.
7 Y. Yan, Q. Cheng, G. Wang and C. Li, *Journal of Power Sources*, 2011, **196**, 7835.
8 Jaidev, R.I. Jafri, A.K. Mishra and S. Ramaprabhu, *Journal of Materials Chemistry*, 2011, **21**, 17601.
9 S. Uppugalla, U. Male and P. Srinivasan, *Electrochimica Acta*, 2014, **146**, 242.
10 B. Singu, U. Male, P. Srinivasan and S. Pabba, *Journal of Solid State Electrochemistry*, 2014, **18**, 1995.
11 L. Wang, X.P. Lu, S.B. Lei and Y.H. Song, *Journal of Materials Chemistry A*, 2014, **2**, 4491.
12 H. Wang, T. Maiyalagan and X. Wang, *ACS Catalysis*, 2012, **2**, 781.
13 T. Kuila, N.H. Kim, D.S. Yu and J.H. Lee, *Carbon*, 2014, **69**, 66.
14 X. Yan, Y. Liu, X. Fan, X. Jia, Y. Yu and X. Yang, *Journal of Power Sources,* 2014, **248**, 745.
15 W. Fan, Y.-Y. Xia, W.W. Tjiu, P.K. Pallathadka, C. He and T. Liu, *Journal of Power Sources*, 2013, **243**, 973.
16 H. Zhang, T. Kuila, N.H. Kim, D.S. Yu and J.H. Lee, *Carbon*, 2014, **69**, 66.
17 H.M. Jeong, J.W. Lee, W.H. Shin, Y.J. Choi, H.J. Shin, J.K. Kang and J.W. Choi, *Nano Letters*, 2011, **11**, 2472.
18 C. Chen, W. Fan, T. Ma and X. Fu, *Ionics*, 2014, **20**, 1489.
19 Y. Qiu, X. Zhang and S. Yang, *Physical Chemistry Chemical Physics*, 2011, **13**, 12554.
20 L. Sun, L. Wang, C. Tian, T. Tan, Y. Xie, K. Shi, M. Li and H. Fu, *RSC Advances*, 2012, **2**, 4498.
21 Z.-S. Wu, A. Winter, L. Chen, Y. Sun, A. Turchanin, X. Feng and K. Muellen, *Advanced Materials*, 2012, **24**, 5130-5135
22 Z. Wen, X. Wang, S. Mao, Z. Bo, H. Kim, S. Cui, G. Lu, X. Feng and J. Chen, *Advanced Materials*, 2012, **24**, 5610.
23 H.-L. Guo, P. Su, X. Kang and S.-K. Ning, *Journal of Materials Chemistry*, 2013, **A 1**, 2248.
24 H. Nolan, B. Mendoza-Sanchez, N.A. Kumar, N. McEvoy, S. O'Brien, V. Nicolosi and G.S. Duesberg, *Physical Chemistry Chemical Physics*, 2014, **16**, 2280.
25 Y. Lu, Y. Huang, F. Zhang, L. Zhang, X. Yang, T. Zhang, K. Leng, M. Zhang and Y. Chen, *Chinese Science Bulletin*, 2014, **59**, 1809.
26 Z.-j. Jiang, Z. Jiang and W. Chen, *Journal of Power Sources*, 2014, **251**, 55.
27 G. Chen, S. Shau, T. Juang, R. Lee, C. Chen, S. Suen and R. Jeng, *Langmuir*, 2011, **27**, 14563.
28 F. Zhang, T. Zhang, X. Yang, L. Zhang, K. Leng, Y. Huang and Y. Chen, *Energy & Environmental Science*, 2013, **6**,1623.
29 Q. Wu, Y. Xu, Z. Yao, A. Liu and G. Shi, *ACS Nano*, 2010, **4**, 1963.
30 S. Zhou, S. Mo, W. Zou, F. Jiang, T. Zhou and D. Yuan, *Synthetic Metals*, 2011, **161**, 1623.
31 M. Zhong, Y. Song, Y. Li, C. Ma, X. Zhai, J. Shi, Q. Guo and L. Liu, *Journal of Power Sources*, 2012, **217**, 6.
32 T.C. Girija and M.V. Sangaranarayanan, *Journal of Power Sources*, 2006, **156**, 705.
33 X. Cui, F. Hu, W. Wei and W. Chen, *Carbon*, 2011, **49**, 1225.
34 D.P. Dubal, D.S. Dhawale, R.R. Salunkhe, S.M. Pawar, V.J. Fulari and C.D. Lokhande, *Journal of Alloys and Compounds*, 2009, **484**, 218.